

Event shape sorting ^{*}

Renata Kopečná¹ and Boris Tomášik^{1,2}

¹ FNSPE, Czech Technical University in Prague, Břehová 7, 11519 Prague, Czech Republic

² Univerzita Mateja Bela, Tajovského 40, 97401 Banská Bystrica, Slovakia

Received: March 22, 2022/ Revised version: date

Abstract. We propose a novel method for sorting events of multiparticle production according to the azimuthal anisotropy of their momentum distribution. Although the method is quite general, we advocate its use in analysis of ultra-relativistic heavy-ion collisions where large number of hadrons is produced. The advantage of our method is that it can automatically sort out samples of events with histograms that indicate similar distributions of hadrons. It takes into account the whole measured histograms with all orders of anisotropy instead of a specific observable (e.g. v_2 , v_3 , q_2). It can be used for more exclusive experimental studies of flow anisotropies which are then more easily compared to theoretical calculations. It may also be useful in the construction of mixed-events background for correlation studies as it allows to select events with similar momentum distribution.

PACS. 25.75.-q Relativistic heavy-ion collisions – 25.75.Gz Particle correlations and fluctuations – 02.50.Ng Distribution theory and Monte Carlo studies

1 Introduction

Hot matter which is created in ultrarelativistic heavy-ion collisions expands very fast in both longitudinal and transverse directions [1,2,3,4]. The expansion is always anisotropic. This is true even in most central collisions, where one would expect symmetry in azimuthal angle due to circular shape of the initial overlap region [5]. In non-central collisions, the overlap of the two colliding nuclei has elliptic shape and thus naturally second-order (and higher even orders) anisotropy in the fireball expansion builds up. On top of this—at any centrality—energy deposition in the interactions of the incoming partons fluctuates and this leads to all orders of anisotropy in the transverse expansion of the fireball. Therefore, even within carefully selected centrality class flow anisotropies vary from event to event [5,6].

Even more degrees of freedom are offered by collisions of deformed nuclei, like uranium. There, the initial anisotropy will also depend on the way how the colliding nuclei are oriented.

This makes the comparison of experimental data to theoretical simulations more complicated, because one has to take into account that every event starts with different initial conditions and evolves differently. Simulations are compared to data in order to pin down the properties of the matter which is being modelled. Initial conditions are unknown, however, although recent hydrodynamic results

indicate that their fluctuations can be directly mapped onto measured fluctuations of hadron distributions [7,8].

Comparison of theory to data must be done with great care so that the spectra of theoretical and experimental fluctuations match each other. Experimentally, events are distributed into centrality classes according to multiplicity. There is a problem with this procedure on the side of theory if very narrow centrality class is demanded, e.g. ultra-central collisions corresponding to 0–0.2% centrality. Events with the same multiplicity may evolve from initial states with different impact parameters¹. Moreover, all those events would differ by the quantum fluctuations in initial energy and momentum deposition [10]. Therefore, events from a class selected according to multiplicity-based centrality may have evolved from different initial conditions and experienced quite different evolution his-

¹ This can be seen, e.g., in Fig. 2 of [9], where the procedure is explained that is used by ALICE collaboration to determine centrality. Within the used Monte Carlo Glauber model if the impact parameter is fixed, then the number of participants may still fluctuate. On the other hand, from the overlap of centrality classes in N_{part} histogram it is clear that fixed N_{part} corresponds to an *interval* of impact parameters. As the experimental multiplicity is determined from multiplicity in a chosen detector, there is yet another source of fluctuation that comes from the uncertainty between multiplicity and N_{part} . In summary, if we fix the multiplicity—even in perfectly spherical nuclei like Pb or Au—there is still some freedom for the impact parameter to fluctuate which we estimate of the order 1 fm. Even more fluctuations can be expected in collisions of non-spherical nuclei, like U.

^{*} Supported in parts by APVV-0050-11, VEGA 1/0469/15 (Slovakia) and MŠMT grant LG13031, SGS15/093/OHK4/1T/14 (Czech Republic).

tory. It would be useful if there was a more selective method to choose events that are more likely to have evolved similarly. In addition to this, in collisions of deformed nuclei the multiplicity itself is definitely not sufficient selection criterion since the same multiplicity may result from events with very different initial *orientations* of the colliding nuclei and thus very different flow patterns. Again, the situation calls for a selection method like the one presented here.

It would thus be advantageous if one could select a collection of events among all measured events (which may or may not belong to the same centrality class) which show very similar distribution of the produced hadrons. For such events one can assume that they also evolved similarly.

The word “similar” when talking about distributions or histograms can be understood in layman’s terms so that they have similar shapes when you rotate them appropriately. There is a possibility how to quantify this with the help of the distance measure in the Kolmogorov-Smirnov test, but this will not be used here because it does not automatically provide a way for sorting. We rather use the Bayesian framework where we basically ask the question: how would the events be grouped, based on the shapes of their histograms.

A method aiming for such event selection has been proposed in [11] and is commonly referred to as “Event Shape Engineering”. It usually employs the size of the flow vector q_n defined on a selection of hadrons from a given event (usually referred to as subevent) as

$$\mathbf{q}_n = \frac{1}{\sqrt{M_s}} \left(\sum_{i=1}^{M_s} \cos(n\phi_i), \sum_{i=1}^{M_s} \sin(n\phi_i) \right), \quad (1)$$

where M_s is the multiplicity of the subevent and ϕ_i are the azimuthal angles of the individual hadrons from the subevent. Events are then selected based on their values of q_n (in most cases q_2). However, only the subevents *not* used in q_n determination can be used in further studies in order to avoid bias.

It is not clear, moreover, whether selecting events according to the value of q_n provides the best possible selection method aimed at collecting similar events. It actually may not be the case, as we demonstrate below.

In this paper we propose the use of a novel method for comparing, sorting and selecting events according to *similarity* with each other. The method is adopted from [12, 13] and was previously used in a different context [14]. Its uniqueness consists in not fixing a single observable which would then be used for sorting of the events. It rather compares complete histograms (e.g. azimuthal angle distributions) of individual events and it sorts the events in such a way that events with similar histogram shapes end up close together. After such a sorting has been performed one simply selects similar events just by choosing a group of events which follow each other in the created series.

On the selected groups of events one could measure various observables (v_n ’s, q_n ’s, radial flow, temperature, ...) which should fluctuate much less than in the whole measured event sample.

A natural application of the method is in construction of correlation functions. There, one often needs a reference distribution which is constructed via the mixed events technique. If events used in mixing are different, this may introduce unwanted artificial effects into the correlation function. Therefore, the mixed events sample is always constructed with aligned event planes. (For application at intermediate energy nuclear collisions see e.g. [15, 16]).

With the help of the proposed method it would be interesting to perform femtoscopic studies where oscillations of radii in azimuthal angle in both second and third order together at the same time should be visible.

We comment more on the applications in the Outlook section.

In the next Section we shall explain the method and in Section 3 we illustrate its use on Monte Carlo data from a toy model. The method is applied on more realistic Monte Carlo data generated by a transport model in Section 4. We conclude in Section 5 and give an Outlook about possible applications of the method and its next development.

2 The method

Suppose that we have a sample consisting of a large number of events. Initially, we can sort and divide those events into N percentiles according to the value of a single observable which can be measured in every event. This can be the value of q_2 , v_2 , multiplicity or any other observable. Generally, we shall refer to this observable as Q . For the sake of clarity let us explain the method with a particular choice: choose $N = 10$ event bins (deciles) and the observable according to which we sort data is $Q = q_2 = |\mathbf{q}_2|$. Let us stress at this point that the method is universal and will not depend on the choice of N and Q .

In each of the event bins we can now produce the histogram of hadron distribution in azimuthal angle summed over all events in the event bin. There is no physics in how the two nuclei are oriented when they collide, and so we have a free choice of how to rotate individual events before adding them to the angle histogram. For the introduction of the method let us align each event according to the second order event plane. Note, however, that the choice of alignment is a sensitive issue which we shall discuss later.

Thus each event is characterized by the bin record of its distribution in azimuthal angle² $\{n_i\}$ and belongs to one of the N event bins which we number with μ . (We shall use Latin letters for angle bins and Greek letters for event bins.)

2.1 Basic relations

Imagine that we take a random event from our big sample and ask an unbiased observer, in which event bin he or she

² We denote n_i the number of particles in angle bin i and the whole record of an event is referred to with the help of braces. Thus summation of all angle bin entries gives the event multiplicity $\sum_i n_i = M$.

thinks that this event belongs. More specifically, we can ask the question in the framework of Bayesian probability: What is the probability³ $P(\mu|\{n_i\})$ that an event with bin record $\{n_i\}$ belongs to the event bin μ ?

This probability will be evaluated with the help of Bayes' theorem

$$P(A|B) = \frac{P(B|A)P(A)}{P(B)}, \quad (2)$$

where $P(A|B)$ is the conditional probability of the event A given event B . The probability of event B can be determined

$$P(B) = \sum_A P(B|A)P(A), \quad (3)$$

where the sum runs over all possible events A . Definitions of symbols $P(B|A)$ and $P(A)$ are analogical.

With the help of Bayes' theorem we can express

$$P(\mu|\{n_i\}) = \frac{P(\{n_i\}|\mu)P(\mu)}{P(\{n_i\})}. \quad (4)$$

Here, $P(\{n_i\}|\mu)$ is the probability that if one randomly draws an event from the distribution function given by average histogram of event bin μ , the result will be the bin record $\{n_i\}$. The prior $P(\mu) = 1/N$ takes the value of 0.1 now. The denominator contains the overall probability of drawing the event $\{n_i\}$ from any of the event bins. It can be determined according to eq. (3)

$$P(\{n_i\}) = \sum_{\nu=1}^N P(\{n_i\}|\nu)P(\nu). \quad (5)$$

The advantage of using the latter formula comes from the fact that we are able to determine $P(\{n_i\}|\nu)$ for each bin record $\{n_i\}$ and every event bin ν

$$P(\{n_i\}|\nu) = M! \prod_i \frac{P(i|\nu)^{n_i}}{n_i!}. \quad (6)$$

Here M is event multiplicity, the product goes over all angle bins i and $P(i|\nu)$ is the conditional probability that random particle falls into angle bin i given that the event to which it belongs stems from event bin ν . It can be determined when we take the number of particles from all events in event bin ν falling into angle bin i . This number is divided by the total number of all particles from events in event bin ν , denoted M_ν

$$P(i|\nu) = \frac{n_{\nu,i}}{M_\nu}. \quad (7)$$

³ Obviously, the event must belong to one of the event bins so that the probabilities must be normalised

$$\sum_{\mu=1}^N P(\mu|\{n_i\}) = 1.$$

When the formula (6) is inserted into (5) and (4) we obtain the practically usable relation from which the large factorials drop out

$$P(\mu|\{n_i\}) = \frac{\prod_i P(i|\mu)^{n_i} P(\mu)}{\sum_\nu \prod_i P(i|\nu)^{n_i} P(\nu)}. \quad (8)$$

With the help of this conditional probability we can determine for an event with angle bin record $\{n_i\}$ its *mean event bin number*

$$\bar{\mu} = \sum_\mu \mu P(\mu|\{n_i\}). \quad (9)$$

2.2 The algorithm

Now we are able to describe the algorithm which is used for sorting of the events.

1. First, all events are sorted according to the observable Q .
2. Events are divided into N event bins according to current sorting.
3. For each event and all event bins the probability $P(\mu|\{n_i\})$ is determined that the event with record $\{n_i\}$ belongs to event bin μ . The mean event number $\bar{\mu}$ is calculated for each event according to (9).
4. Events are sorted again according to their values of $\bar{\mu}$.
5. Events are divided into N event bins according to current sorting.
6. If the new sorting changed assignment of any events into event bins, the algorithm returns to step 3. Otherwise it converged.

The construction of the algorithm is such that once converged, the events are sorted so that those ending up close to each other are characterized by similar angular histograms. This is the best possible experimental approach to the selection of events that have undergone similar evolution. This is as good working definition of what similar events are as it can be.

In the present formulation the average histograms are more strongly determined by high-multiplicity events. Note, however, that the algorithm is independent of event multiplicity. Of course, if in particular physics analysis certain multiplicity is demanded, one can easily use it for event selection and then use the present method for more refined selection of the events.

The final sorting of events also does not depend on the initial sorting. Hence, this method can also be used for a judgment if the particular observable Q , e.g. q_2 or v_2 , is a good measure for selecting similar events. If the initial ordering according to Q is correlated with the final ordering, then the observable Q is good for this purpose. This may not always be the case, as we will show later.

Although the final result does not depend on initial ordering, a good initial ordering can lead to faster convergence of the algorithm.

There is a caveat, however, which has been discussed only shortly so far. The algorithm works well for sorting

Table 1. Parameters used for generating multiplicity dependent v_n .

n	$a_n \times 10^8$	$b_n \times 10^5$	c_n
1	0	0.01667	-0.000680
2	-7.099	20.06	0.07874
3	-2.083	6.658	0.04236
4	-96.38	2.621	0.04897
5	-71.76	2.236	0.01673

histograms in observables that are not periodic, e.g. rapidity. However, the azimuthal angle of particle momentum is a periodic observable, i.e. we can always arbitrarily rotate the events. Practically, two angular histograms may be almost identical when they are both aligned properly, but might appear quite different for the proposed algorithm if they are rotated in random directions. Thus the way how events are aligned initially plays a crucial role and we observed that it strongly biases the final sorting of the events. At the moment we do not have recommendation for an automatic algorithm which would align the events in the best way. Instead, we tested a few reasonable choices for the initial alignment in our toy model studies. With the simple toy model, quite naturally that initial rotation aligning the second-order event planes ψ_2 will lead to sorting characterized by v_2 . Analogically, with aligning the third-order event planes ψ_3 , final sorting is given by v_3 . In the next Section we present results which take into account a combination of both these orderings. That feature was, however, weaker in AMPT-generated events.

3 Illustration of the method

3.1 Elliptic flow

Let us first demonstrate the action of the sorting algorithm on a simple case of events with only first- and second-order anisotropic flow. We generated the azimuthal angles of pions from the distribution

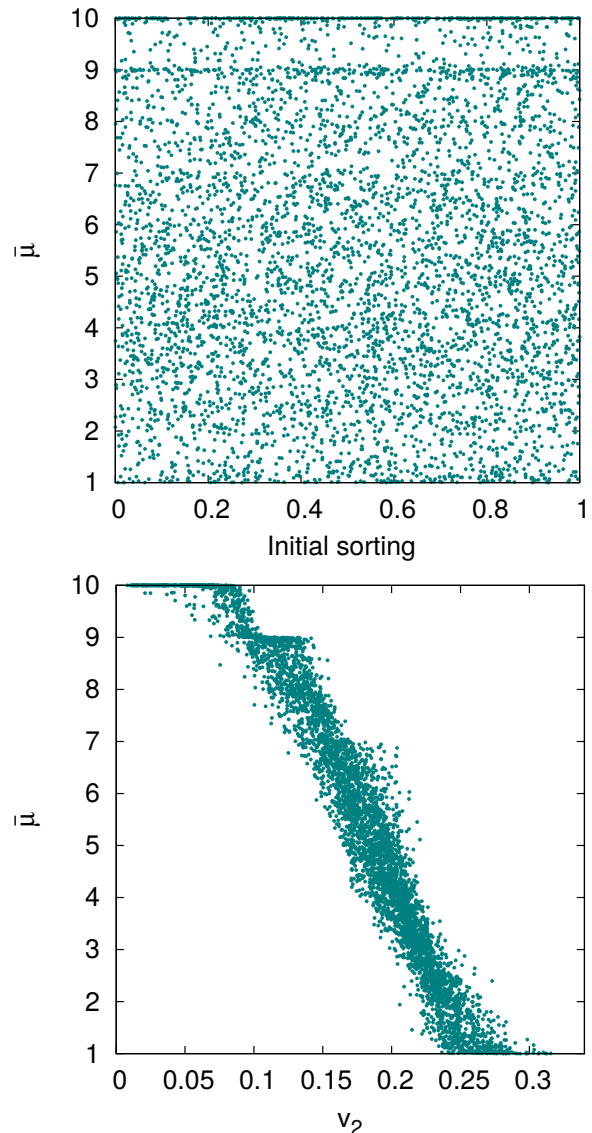
$$P_2(\phi) = \frac{1}{2\pi} (1 + 2v_1 \cos(\phi - \psi_1) + 2v_2 \cos(2(\phi - \psi_2))) . \quad (10)$$

The parameters v_1 and v_2 depend on the multiplicity of the event M as

$$v_n = a_n M^2 + b_n M + c_n , \quad (11)$$

and parameters a_n , b_n , and c_n for each n can be found in Table 1. They have been determined from experimental data as we discuss in Section 3.2. In addition to eq. (11), flow anisotropy parameters v_n are Gaussian-smeared with a width of 0.25. For each event, the directions of event planes ψ_1 and ψ_2 are random and uncorrelated.

We generated 5000 events with multiplicities between 300 and 3000. Directed flow is practically negligible and the dominant anisotropy is second-order. Thus the most reasonable choice of initial event rotation is the alignment

**Fig. 1.** Top: correlation of the resulting sorting variable $\bar{\mu}$ with the initial ordering. Every dot represents one event. Bottom: correlation of $\bar{\mu}$ with v_2 determined for each event via the event plane method.

of second-order event planes defined from the generated Monte Carlo data for each event via

$$q_2 e^{2i\psi_2} = \sum_{j=1}^M e^{2i\phi_j} . \quad (12)$$

To show the power of the method we first ordered the events fully randomly. The algorithm converged after 65 iterations. In Fig. 1 top one can see that the initial ordering indeed has nothing to do with the final ordering of events. In the bottom panel of that Figure we show the correlation of final sorting variable $\bar{\mu}$ with the value of v_2 determined in each event via the event-plane method (results from cummulant method are practically identical). One can clearly see that the ordering is given by the elliptic anisotropy of the particle distribution.

Note that when we started the sorting algorithm with initial ordering according to the value of q_2 in each event, the final correlation was just a mirror image of Fig. 1 bottom. Small values of v_2 corresponded to small $\bar{\mu}$ and high values of v_2 to high values of $\bar{\mu}$. This illustrates that the algorithm always converges to a sorting of events according to their similarity but the direction how they are ordered along $\bar{\mu}$ may be different.

There is a congestion of events seen at $\bar{\mu} = 9$ and 10 in the upper panel of Fig. 1 and a step in the same place in the lower panel of that figure. This actually shows that the sorting was very clear for these two event bins. The congestion is made out of events for which when evaluating $\bar{\mu}$ according to eq. (9), the sum has one clearly dominant term. The probabilities that the event might belong to other event bins are very small.

For illustration, in Fig. 2 we show average histograms of the events in the individual event bins. We see that the relative amplitude of the second order variation (*i.e.* the amplitude divided by the mean value of the bins) decreases from event bin 1 to event bin 10.

The method is thus able to distinguish different shapes of hadron distributions and sort events according to them. In this simple case, this might not look like a big advantage as we could have sorted the events simply by measuring v_2 . Therefore, we proceed with a more complicated example where the algorithm demonstrates its full power.

3.2 Anisotropic flow

We parametrised the dependence of v_n 's on multiplicity through a fit to data from ALICE and ATLAS collaborations [17,18]. Coefficients v_n for $n = 1$ through 5 are parametrised according to eq. (11) with parameters summarised in Table 1.

Then we generated 5000 events with multiplicities between 300 and 3000 pions and angular distributions according to

$$P_5(\phi) = \frac{1}{2\pi} \left(1 + \sum_{n=1}^5 2v_n \cos(n(\phi - \psi_n)) \right). \quad (13)$$

The v_n 's for every event are set by eq. (11) and then smeared with Gaussian distribution with the width of 0.25. The phases ψ_n are selected from uniform distribution and are not correlated with each other.

Now we have to address the question how to rotate the events so that the comparison of individual events to the event bin histograms yields the most reasonable sorting. There are two symmetries at play here: rotational symmetry and parity symmetry. We can rotate an event around the collision axis, and we can also flip it so that we get its mirror image. We have observed that both these symmetries influence the result.

The two dominant components of flow anisotropy are second and third order. Hence, in our tests we focused on the corresponding event planes. If events are all aligned into the direction of second-order event plane, the algorithm becomes sensitive to the second-order anisotropy

and to large extent ignores the third order. Analogically, alignment according to third-order event plane enhances the sensitivity to third order anisotropy. Thus the resulting sorting is rather sensitive to this choice. Furthermore, in both cases the algorithm distinguishes events which look like mirror images of each other (*i.e.* have opposite parity). This must be taken into account when designing the sorting algorithm.

The shape of hadron distribution is never solely determined by v_2 or by v_3 . It rather follows from their combination which is different in every event due to varying phase difference of second and third order event plane. In order to take into account both these components of anisotropy we rotated all events according to the angle bisector between ψ_2 and ψ_3 . We denote its azimuthal angle ψ_{2-3} . Also, in order to take care of the parity symmetry the events were oriented so that ψ_2 is less than $\pi/2$ away from ψ_{2-3} *counterclockwise*.

The initial sorting of the events was random and the algorithm converged after 121 iterations.

From Fig. 3 it is clearly seen that in this case sorting of the events is neither determined by q_2 , nor by v_2 , nor by v_3 . Higher order terms also do not play a big role at all. The event shape is complex and results from an *interplay* of all its simple characteristics. The message of the Figure is that q_2 may not be a good variable to select events according to their shape because panel (a) shows that it is not correlated with the overall shape of the event as soon as more flow harmonics are involved. Note that in our toy model there is neither correlation between the flow harmonics nor between the event planes of different order. This may not be so in real events and then the correlation between sorting variable $\bar{\mu}$ and some of the measured quantities may appear. What we show is thus rather an extreme case. It calls, however, for attention: the overall shape of an event and thus the evolution dynamics running in that event cannot be simplified into a single measured variable. There might be a counterargument that variables like *e.g.* q_2 which are used in Event Shape Engineering are proved to be good at event sorting, because events with different values of q_2 show different values of other measured quantities. However, in addition to this, our method optimizes the sorting so that events which are placed close to each other share as many event shape characteristics as possible. Figure 3 shows that such a sorting may not be connected with any of the commonly used variables.

In Fig. 3 we again observe that the resulting values of $\bar{\mu}$ are grouped around integers. This actually means that the assignment of the events into event bins is very clear, because in determining the value of $\bar{\mu}$ from eq. (9) the probability $P(\mu|\{n_i\})$ is (close to) one for certain μ and (nearly) zero elsewhere. The event then clearly belongs to the event bin μ .

When we tried to start the sorting algorithm with initial ordering according to the value of q_2 it failed to converge within reasonable time (5000 iterations). This happens sometimes when unfavourable initial ordering is used. On the other hand, in other occasions we have checked that also with different initial ordering of events the algo-

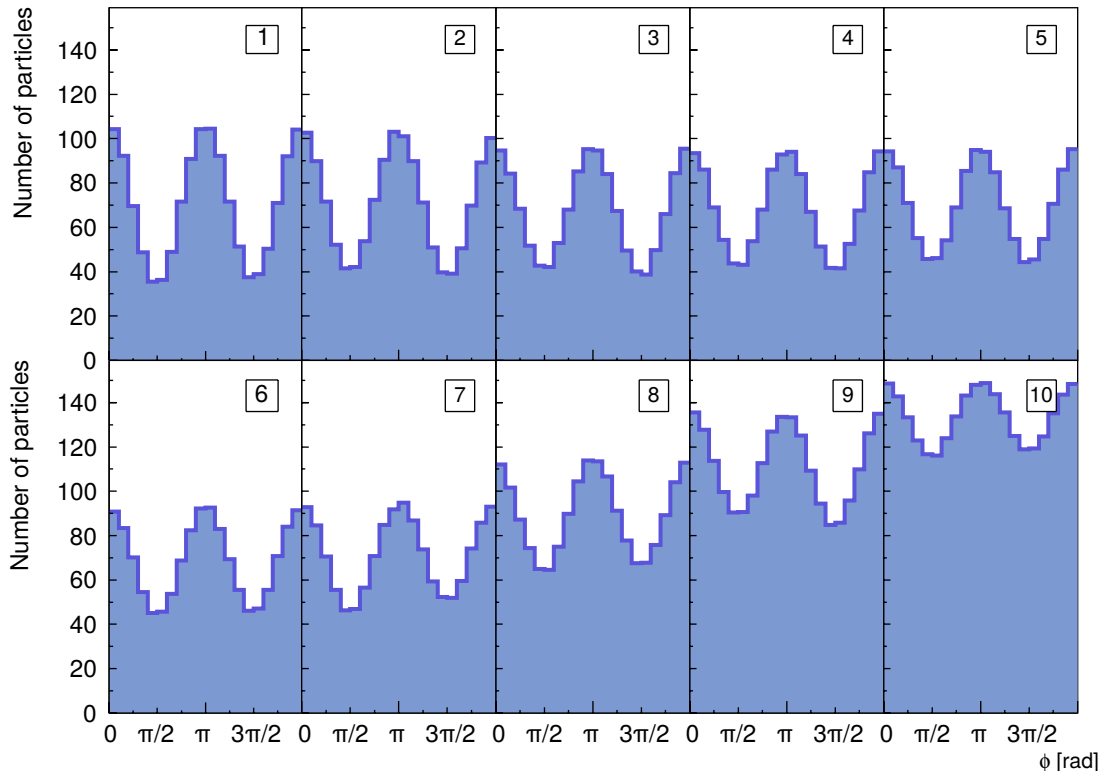


Fig. 2. Average histograms of the azimuthal angles for event bins 1–10, with event bins indicated in the panels. Events with only v_2 and v_1 .

rithm converged to identical final sorting. The only difference could arise from the feature that the algorithm does not follow any specific condition in which direction the events should be sorted. Thus different initial orderings may end up in mutually reversed final orderings.

In Fig. 4 we show the resulting average angular histograms after the sorting. The events indeed differ by their *shape*, not just only by the value of one of the flow harmonics. Since the second and third-order anisotropies are dominant and due to the initial rotation of the events, higher order harmonics are washed out by averaging over the event bins and not seen in the Figure.

A question may appear to what extent the algorithm would sort the events even if they would be drawn from the same distribution. It would still try to place closer together events with similar histograms, and further apart those events with more different histograms. Then—if in doubt—one can test the hypothesis that events are drawn from the same distribution e.g. with the method proposed in [19] or with the help of Kolmogorov-Smirnov test.

4 Application to AMPT events

After we have established and tuned the sorting algorithm, we now use it in a more realistic setting with events generated by the AMPT model [20].

The model was used as commonly distributed with two modifications which are recommended for realistic simu-

lation of Pb+Pb collisions at the LHC collision energy $\sqrt{s_{NN}} = 2.76$ TeV: the parton screening mass was re-set to 2.097 fm^{-1} and the string melting was turned on in order to avoid the underestimation of partonic effects [20].

We have generated 2000 events which correspond to the 0–20% centrality class. On the generated particles we have applied rapidity cut $|y| < 1$ in order to roughly simulate the acceptance of central tracking detectors. For the first rough analysis we have taken all charged hadrons and run the sorting algorithm on them.

The event shapes are dominated by the second order anisotropy, but it is not the only feature that determines the shape of the fireball. When running our sorting algorithm, we have tried three different initial alignments: according to ψ_2 , ψ_3 and ψ_{2-3} . In all three cases only v_2 and q_2 of the events show any pattern of correlation with the final sorting. This is shown in Fig. 5. Surprisingly, even in the case of ψ_3 initial alignment we have found no correlation of final ordering with v_3 . On the other hand, as seen in Fig. 5, there is a pattern that shows that also here the sorting of events is strongly influenced by the second-order anisotropy. It will be interesting in the future to see if this dominance of second-order anisotropy survives also in other centrality classes, particularly in more exclusively selected central event.

It is also interesting to see that in realistic simulation, alignment with respect to ψ_2 does not automatically lead to such a clear correlation of v_2 and $\bar{\mu}$ as it was the case

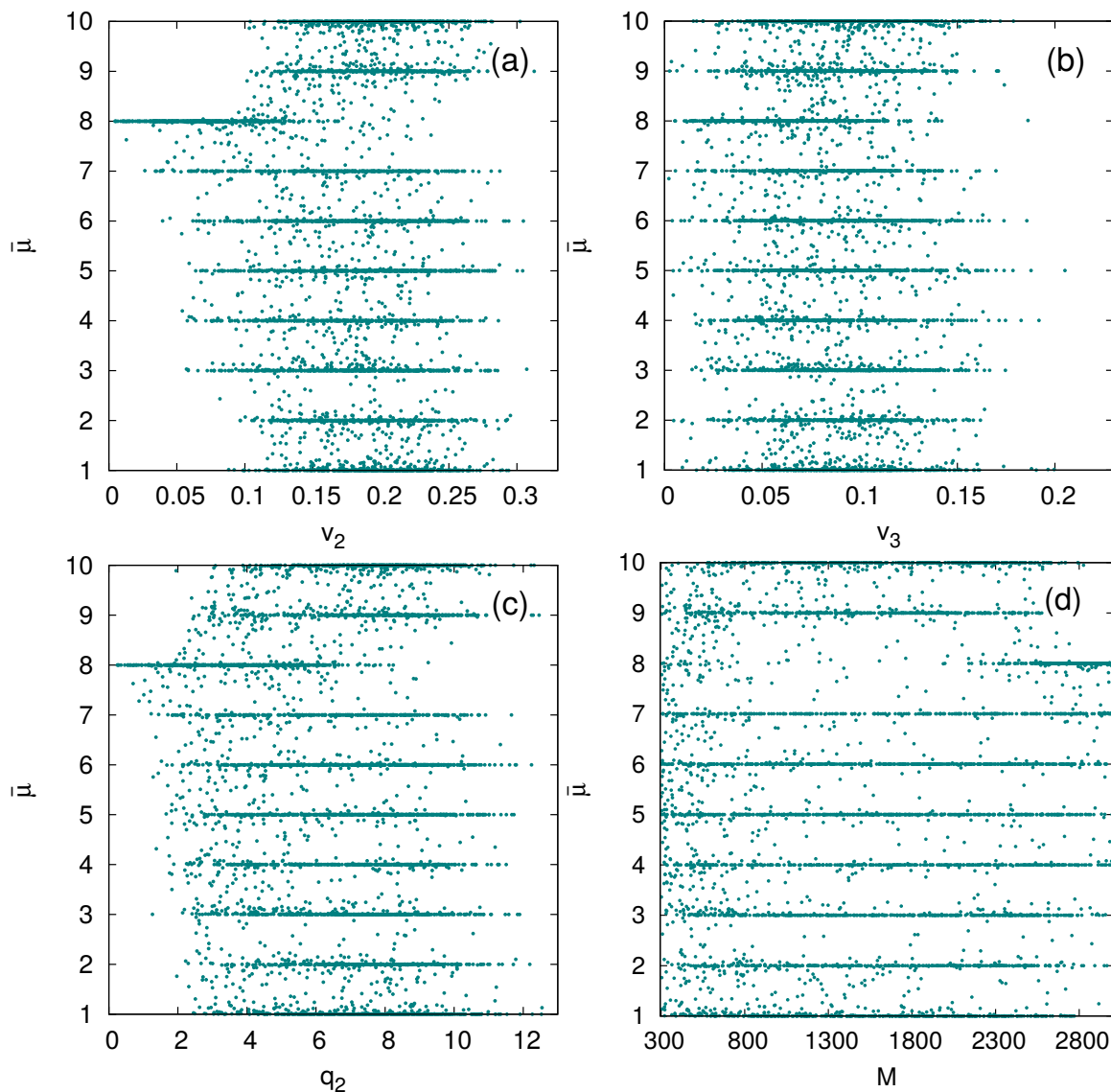


Fig. 3. Correlation of various observables with final sorting variable $\bar{\mu}$. Simulated are events with anisotropies up to 5th order and initial rotation is according to ψ_{2-3} . Correlation with a) v_2 , b) v_3 , c) q_2 , d) event multiplicity.

with our toy model. This is seen in the upper two panels of Fig. 5. Such a correlation exists for the two or three event bins with highest μ 's. There, higher μ corresponds to a higher value of v_2 . However, for $\bar{\mu}$ below 7 there seems to be no correlation between the ordering of the event and v_2 . There is slightly more correlation in case weighted v_2 evaluation, as seen in Fig. 5. We would like to understand where the difference between the events shapes comes from, which forces them into different event bins. To this aim, we show in Fig. 6 the average histograms in individual event bins after the sorting procedure has converged. In event bins 8, 9, and 10 the gradual growth of v_2 is evident. In the other event bins the histograms show a more complicated structure, where higher order anisotropies also give an important contribution. We recall, however, that no clear correlation of any higher v_n with the obtained $\bar{\mu}$ is observed.

The next suspected cause of the difference of events is the relative angle between the directions of \mathbf{q}_2 and \mathbf{q}_3 . We thus studied the correlation between $\bar{\mu}$ and the relative angle. In most cases, no correlation was observed. There is a hint of correlation, though, in case that the events are aligned according to ψ_3 . This is shown in Fig. 7. Indeed, there seems to be a slight correspondence between the assignment to an event bin and the angle between \mathbf{q}_2 and \mathbf{q}_3 . The interpretation is at hand, that for the event shape the relative phase is decisive. Unfortunately, this correlation is gone when we align the events differently. Thus, there are hints that the relative angle is important, but the assignment of an event to an event bin appears to be given by more complicated interplay of various individual features.

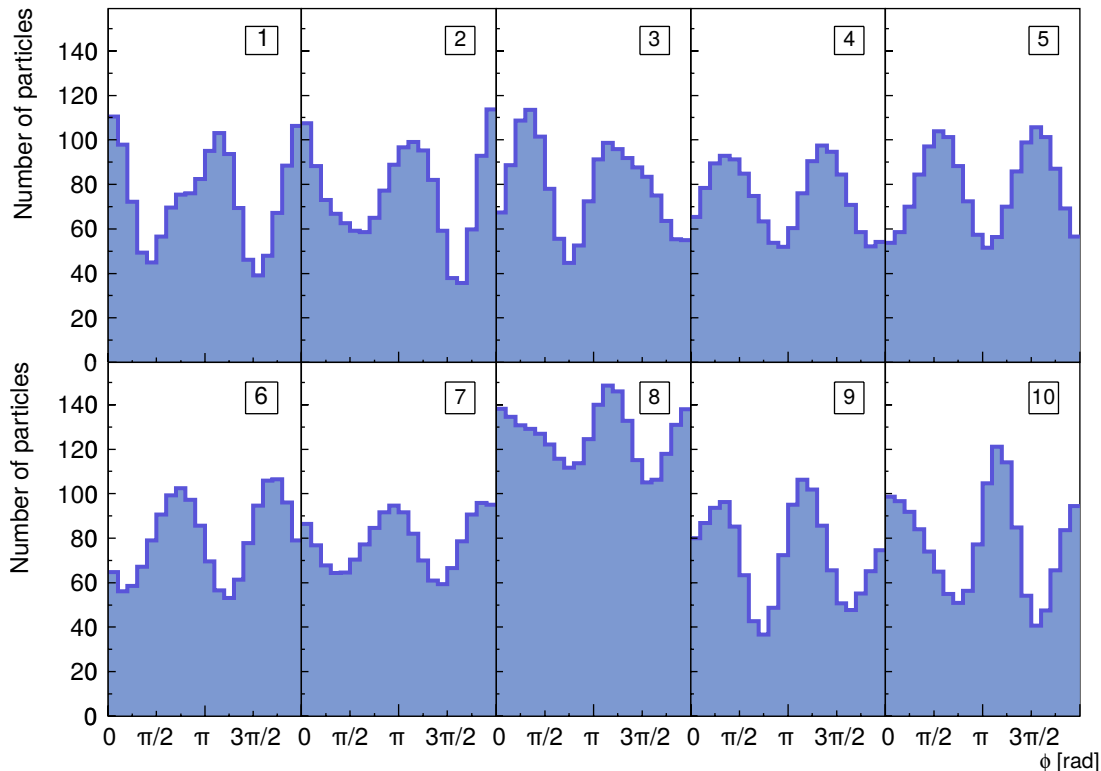


Fig. 4. Average histograms of the azimuthal angles for event bins 1–10, with event bins indicated in the panels. Events with anisotropies up to 5th order.

5 Conclusions and outlook

It is very useful to have a method able to sort events in such a way that it is possible to select those with very similar momentum distribution. One can then assume that they must have undergone similar evolution and this makes it possible to study the dynamics of hot expanding matter more exclusively.

We tested this method on artificial events generated with AMPT. It showed that dividing the events into classes according one selected variable, usually q_2 , does not really correspond to selecting event with the same shapes. It still seems that the main role in determining the event shape—at least for the studied centrality class 0–20%—is played by the second-order anisotropy. Nevertheless, other features are important as well. In one case we could identify the difference $\psi_2 - \psi_3$ to co-determine the assignment to event bins, but this observation is not universal for any initial event alignment and any way of evaluation of q_n 's.

In addition to the explanation of the method of Event Shape Sorting, we thus gave a first superficial study of realistic events with the proposed method. The study of event shapes generated by AMPT for various centralities which would include thorough analysis of all features that influence the final shape and their physics interpretation would go beyond the scope of this work and we plan to publish it in a separate paper.

As was mentioned already in the Introduction, the presented method allows to select groups of events with simi-

lar momentum distributions. If used in data analysis, one can then measure various quantities on such events and study how they are related to the event shape.

The method might even allow to get as close to single-event femtoscopy as possible. First, when doing femtoscopy with a single event one would run into difficulties with the uncorrelated reference distribution which is usually constructed through the event mixing technique. Event shape sorting could provide a selection of events with similar momentum distributions which would make a suitable sample for event mixing. Second, the statistics in a single event would be too small to perform a 3D analysis. However, one could take a sample of events with similar momentum distributions and reasonably expect that they also have the same sizes and undergo the same dynamics. Then, one could analyse the correlation function integrated over the whole selected event sample. The feasibility of such studies will be investigated in the future.

An interesting application appears to be the classification of events from U+U collisions. Due to deformation of the colliding nuclei one expects large fluctuating anisotropies of the transverse flow. Surprisingly, a preliminary study of azimuthally sensitive correlation radii showed no dependence on the value of q_2 [21]. The latter was employed for the selection of events with different final state anisotropy. A short inspection of our Fig. 3c would suggest that this is no surprise at all! As soon as there are other harmonic components of the anisotropy, the shape

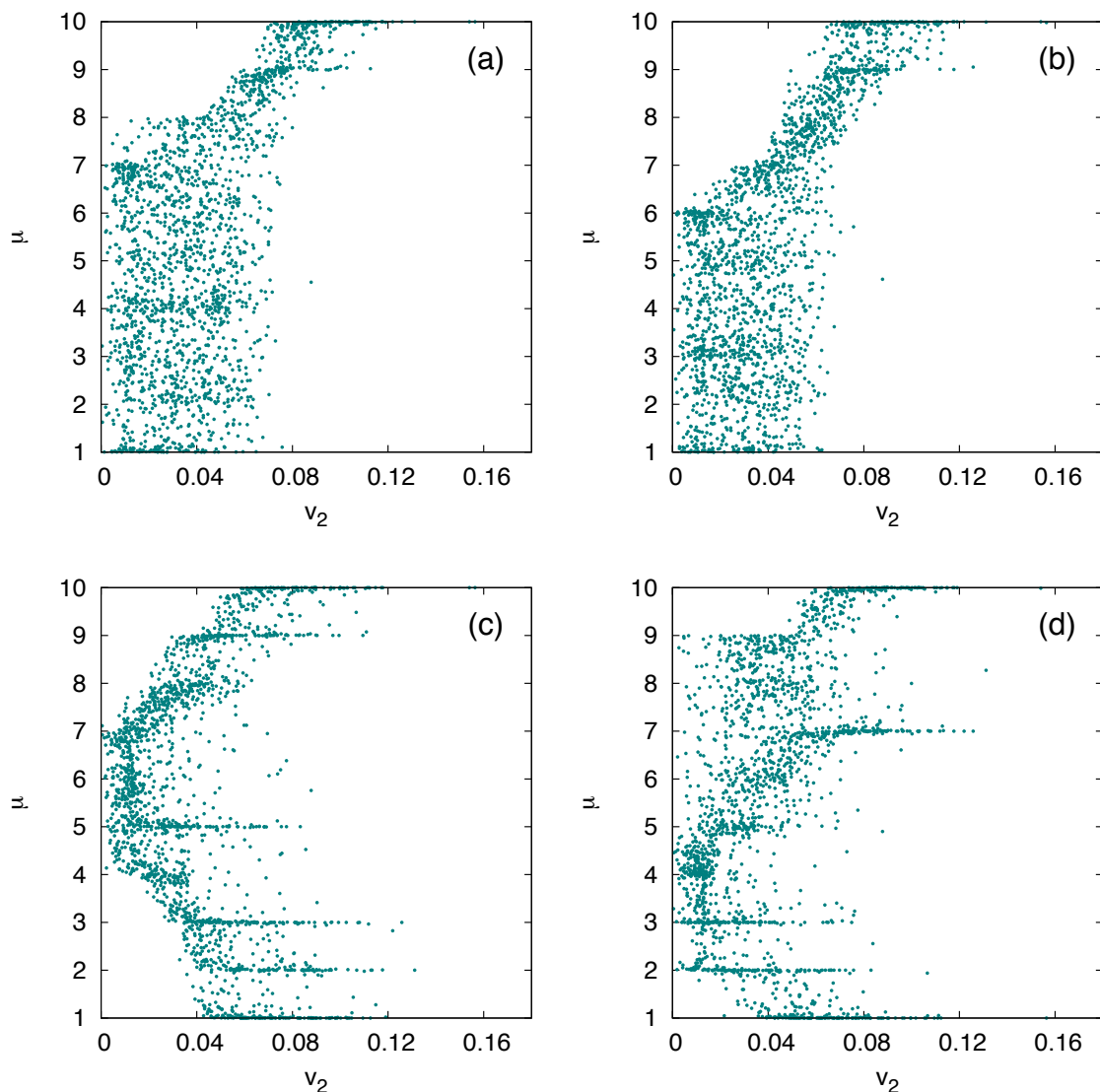


Fig. 5. Correlation of the final sorting variable $\bar{\mu}$ with v_2 of individual events for events generated by AMPT. a) Initial alignment of the events according to ψ_2 , b) initial alignment according to ψ_2 and v_2 evaluated with p_t weight, c) initial alignment according to ψ_3 , d) initial alignment according to ψ_{2-3} .

of the events is more complex. The “proper” partition of events into various classes by the type of anisotropy should be done differently. Our algorithm can do such a proper classification.

Let us also comment again on the interesting though perhaps academic question, how the proposed algorithm would proceed if all events were indeed generated from the same underlying probability distribution and the only differences between them would be due to statistical fluctuations. The algorithm would be sensitive to the differences whatever their cause might be. Thus it would sort the events so that typical fluctuations within one event class would be below the normal statistical ones. Such a situation could be detected with the help of standard statistical tests, like e.g. the Kolmogorov-Smirnov test. In real data we do not expect this to happen, however.

Also, there are still technical issues which require some discussion and will be addressed in the future. Most important is the ambiguity if initial rotation of the events for which we do not yet have optimised rules. Another is the rather high requirement on CPU time for even moderately large event samples. Note however, that we have not tried any fancy computational optimisation of the algorithm so far, and hence we would expect some room for improvement here.

In fact, we also work on a well optimized routine that can readily be taken and applied directly in data analysis. Integration into standard packages like ROOT or HistFitter [22] will be addressed, as well.

In spite of this, we believe that the Event Shape Sorting is worthwhile to apply in real data analysis and carries

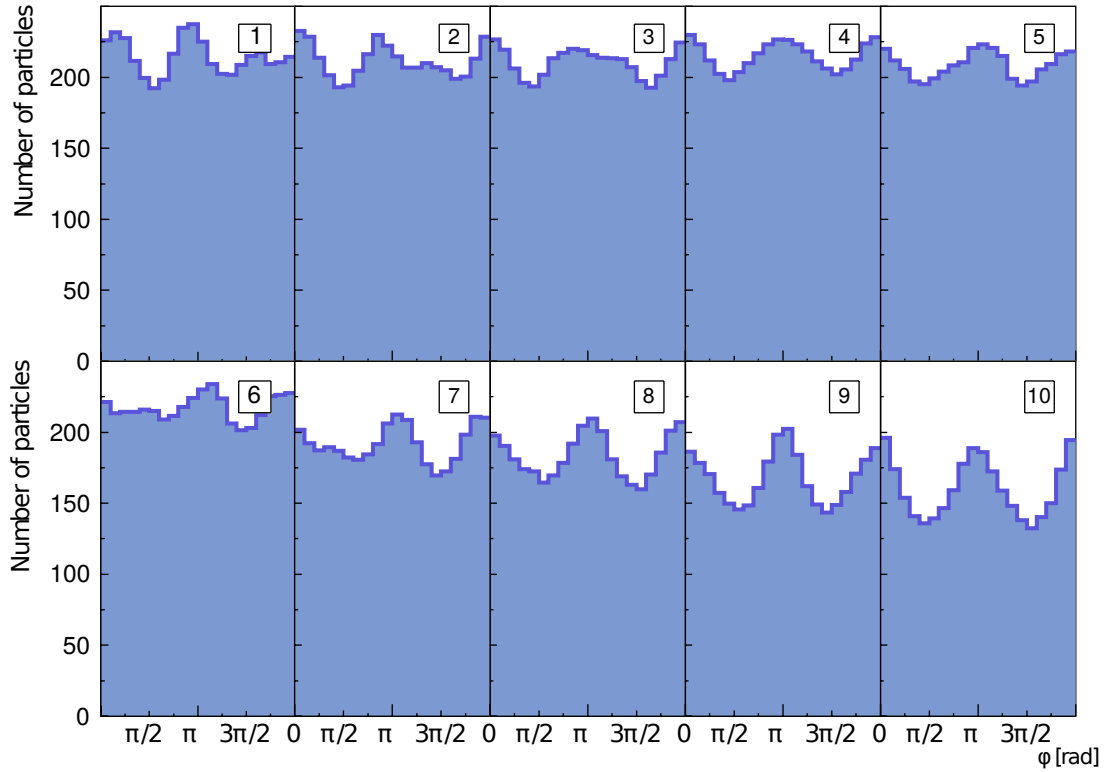


Fig. 6. Average histograms of the azimuthal angles for event bins 1–10, from events generated with AMPT. Initial alignment of events according to ψ_2 .

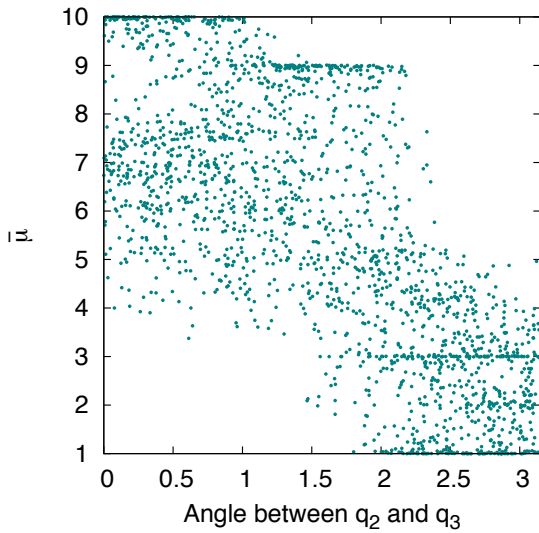


Fig. 7. The correlation of the angle between the flow vectors q_2 and q_3 and the average bin number of the event $\bar{\mu}$. Events aligned according to ψ_3 .

potential to gain us better insight into nuclear dynamics in heavy ion collisions.

Acknowledgement

We are thankful to Sergei Voloshin, Jürgen Schukraft, Arkady Taranenko, and Burkhard Kämpfer for valuable comments and to Serguei Bitjukov for pointing us to Ref. [19]. BT thanks the Frankfurt Institute for Advanced Studies for warm hospitality during his stay where a part of this study was completed.

References

1. I. Arsene *et al.* [PHENIX Collaboration], Nucl. Phys. A **757**, 1 (2005).
2. B.B. Back *et al.* [PHOBOS Collaboration], Nucl. Phys. A **757**, 28 (2005).
3. J. Adams *et al.* [BRAHMS Collaboration], Nucl. Phys. A **757**, 102 (2005).
4. K. Adcox *et al.* [STAR Collaboration], Nucl. Phys. A **757**, 184 (2005).
5. S. Chatrchyan *et al.* [CMS Collaboration], JHEP **02** 88 (2014).
6. G. Aad *et al.* [ATLAS Collaboration], JHEP **11** 183 (2013).
7. H. Niemi *et al.*, Phys. Rev. C **87** 054901 (2013).
8. Ch. Gale *et al.* Phys. Rev. Lett. **110** 012302 (2013).
9. B. Abelev *et al.* [ALICE Collaboration], Phys. Rev. C **88** 044909 (2013).
10. C. Shen, Z. Qiu and U. Heinz, arXiv:1502.04636 [nucl-th].
11. J. Schukraft, A. Timmins, S. Voloshin, Phys. Lett. B **719** 394 (2013).

12. S. Lehmann, A.D. Jackson, B. Laustrup, arXiv:physics/0512238
13. S. Lehmann, A. D. Jackson and B. E. Laustrup, *Scientometrics* **76** 369 (2008) [physics/0701311 [physics.soc-ph]].
14. S. Lehmann, A.D. Jackson, B. Laustrup, *Nature* **444** 1003 (2006).
15. B. Kämpfer *et al.*, *Phys. Rev. C* **48** R955 (1993).
16. R. Kotte *et al.*, *Phys. Rev. C* **51** 2686 (1995).
17. G. Eyyubova [for the ALICE Collaboration], *EPJ Web of Conferences* **70** 00075 (2014).
18. G. Aad *et al.* [ATLAS Collaboration], *Phys. Rev. C* **86** 014907 (2012) [arXiv:1203.3087 [hep-ex]].
19. S. Bityukov, N. Krasnikov, A. Nikitenko and V. Smirnova, *Eur. Phys. J. Plus* **128** 143 (2013) [arXiv:1309.4649 [physics.data-an]].
20. Z.-W. Lin *et al.*, *Phys. Rev. C* **72** 064901 (2005)
21. J. Campbell [for the STAR Collaboration], poster at the conference Quark Matter 2014, Darmstadt, Germany, May 19-24, 2014.
22. M. Baak, G. J. Besjes, D. Côte, A. Koutsman, J. Lorenz and D. Short, *Eur. Phys. J. C* **75** 153 (2015) [arXiv:1410.1280 [hep-ex]].